ORIGINAL RESEARCH

RETRACTED ARTICLE: siRNA-loaded poly(histidine-arginine)6-modified chitosan nanoparticle with enhanced cell-penetrating and endosomal escape capacities for suppressing breast tumor metastasis

Ping Sun[1]
Wei Huang[1]
Lin Kang[1]
Mingji Jin[1]
Bo Fan[1]
Hongyan Jin[2]
Qi-Ming Wang[1]
Zhonggao Gao[1]

[1]State Key Laboratory of Bioactive Substance and Function of Natural Medicines, Department of Pharmaceutics, Institute of Materia Medica, Chinese Academy of Medical Sciences and Peking Union Medical College, Beijing, [2]Yanbian University Hospital, Jilin, People's Republic of China

Abstract: An ideal carrier that delivers small interfering RNA (siRNA) should be designed based on two criteria: cellular-mediated internalization and endosomal escape. Poly(histidine-arginine)6(H6R6) peptide was introduced into chitosan (CS) to create a new CS derivative for siRNA delivery, 6-polyarginine (R6) as cell-penetrating peptides facilitated nanoparticle cellular internalization has been proved in our previous research, and 6-polyhistidine (H6) mediated the nanoparticle endosome escape resulted in the siRNA rapid releasing into tumor cytoplasm. H6R6-modified CS nanoparticles showed a higher transfection efficiency and better endosomal escape capacity compared to ungroomed CS nanoparticle in vitro. Noticeably, H6R6-modified CS nanoparticles effectively inhibited tumor cell growth and metastases in vivo and significantly improved survival rate. Therefore, we concluded that H6R6-modified CS copolymer can act as an ideal carrier for siRNA delivery and as a promising candidate in breast cancer therapy.

Keywords: poly(histidine-arginine)6-peptide-modified chitosan nanoparticle, cell-penetrating peptide, endosome/lysosome escape, gene delivery, breast carcinoma

Abbreviations

CLSM, confocal laser scanning microscopy; CPPs, cell-penetrating peptides; CS, chitosan; CS-NP, chitosan nanoparticle; EDC, carbodiimide hydrochloride; FBS, fetal bovine serum; H&E, hematoxylin and eosin; H6, polyhistidine composed of six histidines; H6R6, poly(histidine-arginine)6; H6R6-CS, poly(histidine-arginine)6-modified chitosan; H6R6-NP, poly(arginine-histidine)6-modified chitosan/siRNA nanoparticles; HOBt, 1-hydroxybenzotriazole monohydrate; MTT, 5-diphenyltetra-zolium bromides; OD, optical density; PBS, phosphate-buffered saline; PI, propidium iodide; R6, polyarginine composed of six arginines; siRNA, small interfering RNA.

Introduction

In recent years, the morbidity of breast carcinoma has increased; however, it is difficult to treat breast carcinoma in the clinical setting because of its high metastasis rate and high drug resistance to traditional chemotherapy.[1,2] Gene therapy is being effectively used in the treatment of various malignant tumors due to its excellent features such as high specificity and relative low toxicity.[3,4] Survivin is an important member of the inhibitors of apoptosis protein family, and a number of studies had reported that survivin gene was highly overexpressed in breast cancer, which was closely correlated with the diagnosis,

Correspondence: Zhonggao Gao;
Wei Huang
State Key Laboratory of Bioactive Substance and Function of Natural Medicines, Department of Pharmaceutics, Institute of Materia Medica, Chinese Academy of Medical Sciences and Peking Union Medical College, 1 Xian Nong Tan Street, Beijing 100050, People's Republic of China
Tel/fax +86 10 6302 8096
Email zggao@imm.ac.cn;
huangwei@imm.ac.cn

submit your manuscript | www.dovepress.com

Dovepress

[facebook] [twitter] [linkedin] [youtube]

http://dx.doi.org/10.2147/IJN.S129436

International Journal of Nanomedicine 2017:12 3221–3234

3221

therapy, and prognosis of breast cancer.[5] Therefore, survivin gene is generally chosen as a target site in breast cancer therapy, because inhibition of survivin gene can effectively induce tumor cell apoptosis and further suppress the growth of tumor.[6,7] Using siRNA as a therapeutic drug to silence survivin gene effectively inhibits the growth and metastasis of breast cancer cells.[8,9] However, in order to siRNA be applied in the clinical setting, various challenges including physiological barriers such as serum ribonucleases degradation, renal clearance, low cellular uptake efficiency, and poor endosomal escape after endocytosis have to be overcome.[10–15] Development of a suitable carrier that effectively delivers siRNA to tumor cells is crucial to enhance its therapeutic efficiency.

Generally, in gene therapy, CS and its derivatives are used to deliver nucleic acid because of its non-toxic, non-immunogenic, biodegradable, biocompatible characteristics. CS with cationic charge due to the presence of primary amine group in weak acid environment is liable to form nanoparticles (NPs) or complexes with siRNA through electrostatic interactions. Therefore, CS-NP has an excellent potential to deliver targeted survivin siRNA into tumor cells.[16,17] However, the application of CS as a vector for therapeutic siRNA delivery is limited due to its low transfection efficiency and poor cell membrane-penetrating capacity thereby resulting in poor CS-NP uptake by tumor cells. Moreover, as CS has poor buffering capacity, it cannot mediate endosome/lysosome escape, and a part of CS-NP captured by endosomal/lysosomal system is degraded by lysosomal enzymes. All these drawbacks make CS-NP an inefficient candidate in cancer treatment.[19,20] To overcome these drawbacks, CS is modified by a number of chemical and biological materials[21–23] to obtain CS derivatives; these derivatives have an enhanced transfection efficiency for siRNA delivery.

CPPs are usually used in pharmaceuticals as potential membrane-penetrating biomaterials. They can facilitate cellular internalization of macromolecules such as proteins, nucleic acids, and liposomes by interacting with negatively charged plasma membrane.[24] Currently, hundreds of CPPs have been reported including natural polypeptides such as TAT peptide and artificially synthesized polypeptides. Few studies have found that artificially synthesized CPP sequences contain abundant of arginines,[25,26] and the penetration efficiency of arginine-rich CPPs are more effective compared to arginine-poor CPP peptides. Therefore, arginine-rich peptides are most frequently used as CPPs. Due to its strong positive charge, arginine has an excellent cell-penetrating efficiency. As a result CPPs also have an excellent cell-penetrating efficiency, and a variety of

polyarginine sequences have been determined, for example, 6-polyarginine (R6), 8-polyarginine, and 9-polyarginine.[27–29] The poly-arginines were introduced into carriers to improve their transfection efficiency for DNA or siRNA delivery, so CPPs-modified delivery vector with higher cellular uptake can transport DNA or siRNA into tumor cells easily.

In addition, to increase transfection efficiency, siRNA-loaded NPs must escape the endosome/lysosome pathway after intracellular uptake. Histidine modified the siRNA delivery carriers to improve its buffer ability.[30,31] Histidine aids in endosomal/lysosomal due to its buffering capacity. This buffering capacity results in a "proton sponge effect" and destabilizes the membranes of the endosome/lysosome in the acidic environment and allow the NPs or complexes to escape from the endosome/lysosome rapidly.[32–34] In this study, we incorporated histidine residues into 6-polyarginine to design a novel H6R6 peptide to increase intracellular uptake and help NP escape from the endosome/lysosome and to enable the abundant release of siRNA into the cytoplasm to increase its bioavailability.

Based on this theory, in our study, H6R6 peptide was introduced into CS to obtain a new H6R6-CS copolymer as siRNA delivery vector. H6R6-CS copolymer possesses higher cellular internalization efficiencies and an outstanding buffering capacity compared to ungrouped CS; therefore, H6R6-CS/siRNA nanoparticles (H6R6-NP) showed a higher cellular uptake efficiency due to the presence of R6 that acted as CPPs to improve the cellular internalization of NPs and H6 producing "proton sponge effect" in the endosome/lysosome, can assist NPs to mediate lysosome/endosomal escape to further enhance transfection efficiency. This scheme is shown in Figure 1.

Materials and methods
Materials, cells cultures, and animals
CS (degree of deacetylation 88%) was obtained from Zhejiang Golden Shell Pharmaceutical Co., Ltd (Zhejiang, People's Republic of China). H6R6 peptide was synthesized by Zhongke Yaguang Biological Technology Co., Ltd (Beijing, People's Republic of China). siRNA was purchased from GenePharma Co., Ltd (Suzhou, People's Republic of China). HOBt and EDC were obtained from Aladdin Company (Shanghai, People's Republic of China). MTTs were obtained from Sigma Aldrich (St Louis, MO, USA). Cell Navigator™ Lysosome Staining Kit was purchased from AmyJet Scientific Inc (Beijing, People's Republic of China). Luciferase Assay Kit was purchased from Promega Corporation (Madison, WI, USA). Annexin V-FITC/PI apoptosis detection kit was
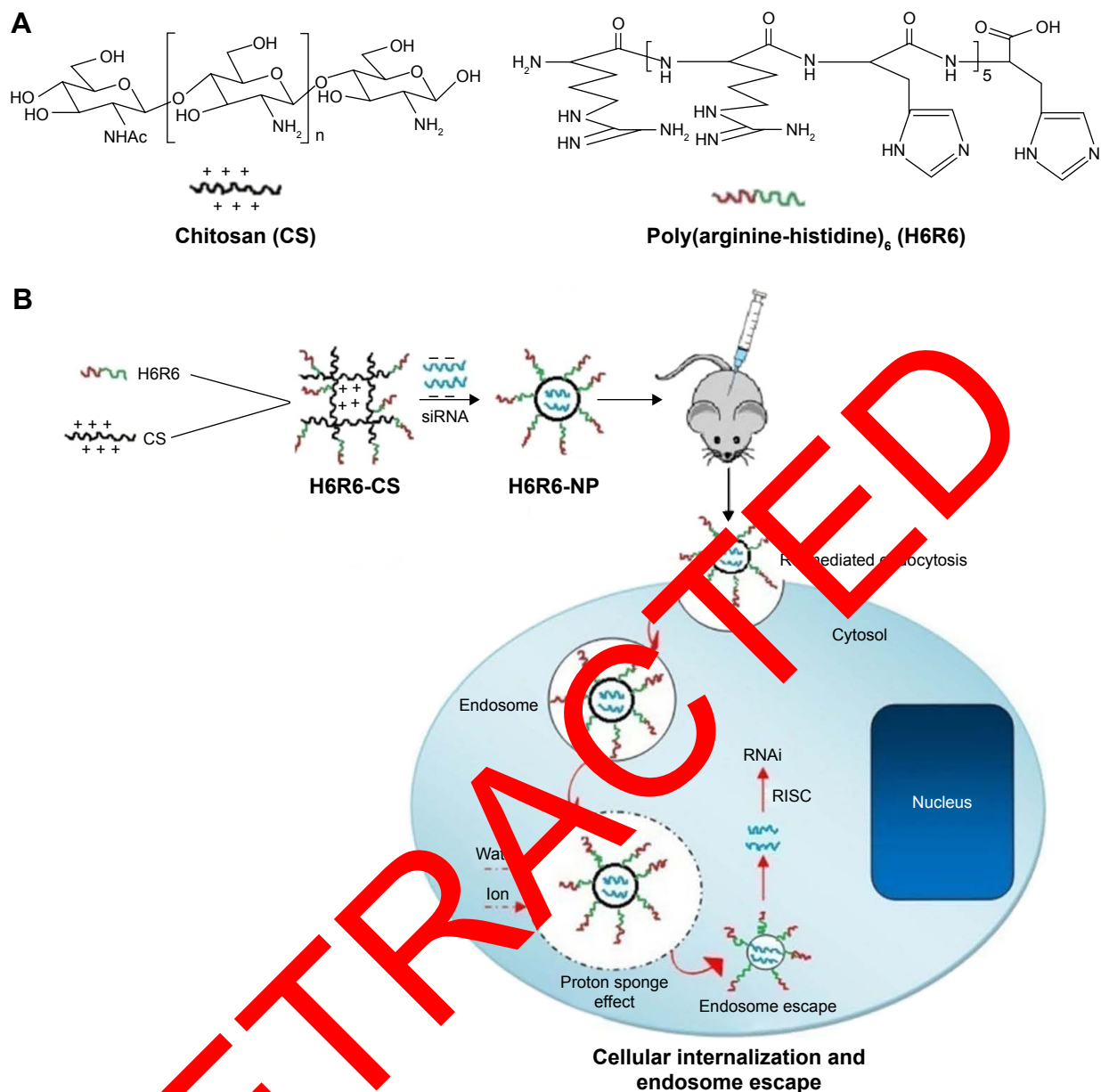
Figure 1 The process of intracellular behavior of H6R6-NP.

Notes: (**A**) The structural formulas of CS and H6R6 peptide. (**B**) The process of endosomal escape of H6R6-NP.

Abbreviations: H6R6-NP, poly(histidine-arginine)₆-modified chitosan/siRNA nanoparticles; siRNA, small interfering RNA; H6R6-CS, poly(histidine-arginine)₆-modified chitosan; R6, polyarginine composed of six arginines; RISC, RNA-induced silencing complex.

obtained from the Key Gen Biotech (Nanjing, People's Republic of China). RPMI-1640 medium, DMEM medium, FBS, 0.25% trypsin, and PBS were all purchased from Thermo Fisher Scientific Inc (Waltham, MA, USA).

4T1 cells were obtained from the Department of Pathology, Institute of Medicinal Biotechnology, Peking Union Medical College, which was maintained with RPMI-1640 medium containing 10% FBS at 37°C in 5% CO_2 incubator. Female BALB/c mice (4–6 weeks old) were purchased from Laboratory Animals Center of Vitalriver (Beijing, People's Republic of China), which were fed in specified experimental animal

room. All animal experiments were approved by the Laboratory Animal Ethics Committee, Institute of Materia Medica, Chinese Academy of Medical Sciences and Peking Union Medical College. The operational procedures of all animal experiments complied with institutional guidelines and protocols for the care and use of experiment animals.

Synthesis and characterization of H6R6-CS copolymer

H6R6-CS copolymers were synthesized by couple-crosslinking method and the procedure is as follows. Briefly,

H6R6 peptide was dissolved in 5 mL DMF solution, and coupling reagents containing EDC, HOBt, and triethylamine were added. To this mixture CS was added and allowed to react for 24 h to obtain the copolymer. After 24 h, the reaction mixture was purified by dialysis for 48 h (molecular weight cutoff =3,500 Da) using distilled water so as to remove the unreacted peptides and DMF. The dialyzed mixture was then freeze-dried and H6R6-CS copolymer was obtained. The molecular structures of H6R6-CS copolymers were determined by mercury 500 MHz ^{1}H-NMR, and the samples were dissolved in 2% CF_3COOD/D_2O at a concentration of 5 mg/mL.

Preparation and characterization of H6R6-NP

H6R6-NP was prepared by complex coacervation method as previously reported in the literature.[35,36] H6R6-CS polymer was dissolved in acetic acid buffer solution whose pH is 5.5 and then the mixture was filtered using 0.22 mm sterile membrane. siRNA solution was obtained by diluting 20 μM siRNA in DEPC water. Then the H6R6-CS copolymer solution and free siRNA solution were heated in a water bath for 20 min at 55°C, and subsequently mixed and vortexed for 40 s to obtain H6R6-NP.

The particle size and zeta potential of H6R6-NP were measured by Malvern Zetasizer Nano instrument, and the surface morphology of H6R6-NP was detected using transmission electron microscopy.

Evaluation of binding affinity of H6R6-CS copolymer to siRNA

The complexation behavior of H6R6-CS copolymer with siRNA was studied by agarose gel electrophoresis. H6R6-NPs were prepared in different weight ratios ranging from 60:1 to 200:1. Naked siRNA of same ratios was considered as control group. H6R6-NP associated with 1 μg of siRNA was loaded in an agarose gel well (4% agarose gel), and electrophoresis was carried out at a constant voltage of 80 V for 30 min in 1% TAE buffer solution. The agarose gel was then stained with ethidium bromide solution for 60 min. The siRNA bands formed were analyzed using UV gel image system (SIM135A, SIM International Group Co. Ltd) at a wavelength of 365 nm.

Cytotoxicity analysis of H6R6-CS copolymer

The cytotoxicity of H6R6-CS copolymer and anti-proliferation effect of H6R6-NP in vitro were analyzed by MTT

assay. 4T1 cells (5,000 cells/well) and B16-F10 cells (8,000 cells/well) were used in this assay and they were seeded into each well of 96-well plates and incubated with RPMI-1640 and DMEM medium, respectively. Then, the cells were treated with different concentrations of H6R6-CS copolymers (5–80 μg/mL) for 4 h in a serum-free medium, and the medium was replaced with fresh medium containing 10% FBS and incubated for another 44 h. Then, the culture medium was removed carefully and washed with PBS twice. Subsequently, 4T1 cells and B16-F10 cells were incubated with MTT solution for 4 h, and then 150 μL DMSO was added to dissolve the intracellular formazan crystals. The OD was detected by a microplate reader at 490 nm. Cell viability (%) was defined using the following formula: viability (%) = $(OD_{sample}/OD_{control}) \times 100\%$, where OD_{sample} is the OD obtained in the presence of copolymer and $OD_{control}$ is the absorbance of cells that were not treated with copolymer.

Cytotoxicity analysis of H6R6-NP

To analyze the cytotoxicity of H6R6-NP, 5×10^3 4T1 cells were seeded into 96-well plates and incubated for 24 h for adherence. H6R6-NP at concentrations ranging from 2.5 to 10 pmol/well was added to the cells in serum-free medium. The treated cells were cultured for 24 h and 48 h, respectively, and then the cell viability was measured at 490 nm using a microplate reader.

To further estimate the anti-proliferation effect of H6R6-NP on 4T1 cells, 5×10^3 4T1 cells were seeded into 96-well plates and incubated for 24 h for adherence. The cells were then incubated with naked siRNA, CS-NP, H6R6-NP, and Liposome 2000 for 48 h. The concentration of siRNA in every group was 5 pmol/well, and the cell viability was tested by a microplate reader.

Wound-healing assay

The anti-metastasis effect of H6R6-NP was estimated using a wound-healing assay. 5×10^4 4T1 cells were seeded into 24-well plates, incubated overnight in 5% CO_2 incubator for adherence, and scraped with the aid of sterilized tips to create a linear scratch wound. The cells were then washed twice with PBS solution carefully. A total of 20 μL H6R6-NP suspension containing 30 pmol/well siRNA and 480 μL fresh serum-free medium were added to every well. Naked siRNA (30 pmol/well) and CS-NP (30 pmol/well) were used as negative control, and cells that did not undergo any treatment were used as blanks. Movement of cells into the wound area was photographed at 0 h, 24 h, and 48 h using an inverted microscope and digital camera.

Cellular uptake study

The apoptosis effect and cellular uptake of H6R6-NP were evaluated by flow cytometry. To evaluate cell apoptosis, 8×10^4 4T1 cells were seeded into 6-well plates with RPMI-1640 medium supplemented with 10% FBS and incubated overnight before transfection. The medium was then removed and H6R6-NP solution containing 200 pmol siRNA in a serum-free medium was added. After 4 h of incubation, it was replaced by fresh cell culture medium containing 10% FBS. The treated cells were further incubated for another 44 h at 37°C in 5% CO_2 incubator. After incubation, the cells were washed three times with PBS, trypsinized by 0.25% trypsin, and centrifuged at a speed of 2,000 rpm for 5 min. The collected cells were suspended in 300 µL binding buffer solution, and 5 µL Annexin V-FITC and 5 µL PI were added to the above solution. After 10 min of incubation at room temperature, the treated cells were detected by flow cytometer.

Induced apoptosis assay

To evaluate the uptake efficiency of H6R6-NP, 4T1 cells were seeded into 12-well plates at a density of 15×10^4 cells/well with RPMI-1640 containing 10% FBS. After 24 h of incubation for proliferation to take place, the cells were transfected with H6R6-NP solution containing 100 pmol/well siRNA-FAM in a serum-free medium for 4 h. The same concentration of naked siRNA and CS-NP were treated control group. The cells that did not undergo any treatment were treated as blank group. After 4 h of transfection, the medium was removed and the cells were washed with PBS twice, digested with 0.25% trypsin, and the cells were collected in 0.5 mL PBS solution. The uptake behavior of the NPs was analyzed by flow cytometry.

CLSM analysis

4T1 cells were seeded into 24-well plates at a density of 3×10^4 cells/well in RPMI-1640 containing 10% FBS and allowed to adhere overnight. The cells were treated with naked siRNA-FAM, CS-NP, and H6R6-NP in a serum-free medium for 4 h. After 4 h incubated, the 4T1 cells in every group were washed with PBS twice, subsequently, were fixed in 4% formaldehyde for 10 min, and stained cell nuclei with DAPI for 10 min, then, were observed using confocal fluorescence microscope (LSM710) at the 410–495 nm filters.

Endosomal escape ability of H6R6-NP

The ability of endosomal escape of H6R6-NP was investigated by CLSM. In brief, 4T1 cells were seeded into 24-well plates at a density of 4×10^4 cells/well and incubated overnight. The cells were then treated with CS-NP and H6R6-NP in a serum-free medium for 6 h, respectively. After 6 h incubated, the 4T1 cells in CS-NP and H6R6-NP group were washed three times with PBS and fixed in 4% formaldehyde for 10 min, stained cell nuclei with DAPI for 10 min, and stained endosome/lysosome with lysosomal-staining solution for 60 min at room temperature, then cells were washed with PBS solution again and observed through the confocal fluorescence microscope (LSM710).

Suppression of tumor growth and metastasis

4T1[luc] cells in log phase of growth were suspended in PBS solution. A total of 0.1 mL of the suspension solution was subcutaneously injected into the fourth mammary fat pad of BALB/c female mice (4–6 weeks old). Two weeks after the inoculation of 4T1 cells, the volume of the solid tumor grew to 130–140 mm³. The tumor-bearing mice were randomly divided into three groups each containing five animals: blank (saline), naked siRNA, H6R6-NP. In naked siRNA and H6R6-NP groups, siRNA was injected regularly every other day for five times at a concentration of 0.5 mg/kg. The tumor volume was measured periodically using a caliper ruler and calculated by the following equation: tumor volume $(mm^3) = (L \times S^2)/2$, where S and L represent the short and long diameter of tumor, respectively. All mice were executed by cervical dislocation, the tumors and organs (lung and liver) excised, and then immersed in 4% (w/v) paraformaldehyde solution for histopathological analysis.[37] The lung and liver tissues of tumor-bearing mice were excised and fixed in 4% (w/v) paraformaldehyde solution for 2 days, and the tissue samples of the lung and liver were embedded into paraffin, followed by staining with H&E. The stained sections were observed and photographed using light microscopy.

Animal survival experiment

To investigate the survival ratio of tumor-bearing mice, 20×10^4 4T1 cells were subcutaneously injected into the fourth mammary region of 4–6-weeks-old female BALB/c mouse. These mice were treated as tumor-bearing mice model. After the tumor volume reached about 130 mm³, the mice were then randomly assigned to three groups (n=10): the test group was injected with H6R6-NP and blank group was injected with 0.9% saline. The negative group was injected with equal dose of naked siRNA. Drug administration was carried out every other day for five times and the injection dose of siRNA was

0.3 mg siRNA/kg. The survival ratio of tumor-bearing mice was observed on time.

Results and discussion
Synthesis and characterization of H6R6-CS copolymer

H6R6-CS copolymers were prepared by link-coupling method and the steps are as follows. First, H6R6 peptide was activated at room temperature, and EDC and HOBt were used as coupling agent. CS was then added to the solution and was allowed to reacting for 24 h to obtain H6R6-CS copolymers. As we preconceived, H6R6 peptide was introduced into the CS molecule. This design improved the transfection efficiency and had two advantages: R6 helped the NPs to penetrate the cell biomembrane resulting in a high uptake efficiency and H6 helped the NPs to escape from endosome/lysosome due to its protonation in the acidic environment. Therefore, this synthetic H6R6-CS copolymer is an outstanding carrier for siRNA delivery.

The ¹H-NMR spectra of H6R6-CS copolymer is shown in Figure 2. The chemical signal at 1.7–1.8 ppm belonged to CS appeared at 1.7–1.8 ppm, which belonged to the *N*-acetylated units proton (–COCH₃) from CS, and the multiple peaks at

3.2–3.6 ppm belonged to the glucosamine units from CS (H-3 to H-6, H-6′) (Figure 2A).[38] Characteristic peaks of H6R6 peptides were also observed: the multiple peaks at 1.1–1.5 ppm were attributed to -NH₂-CH₂-of arginine, and the protons peaks at 7.0 ppm and 8.3 ppm were assigned to the protons of imidazole ring from histidine shown in Figure 2B.[39,40] The characteristic peaks of H6R6 peptide and CS that simultaneously appeared in the ¹H-NMR spectra of H6R6-CS copolymer indicated that H6R6 peptides were successfully grafted to the surface of CS molecule (Figure 2C). The number of conjugated H6R6 peptide was calculated by comparing ¹H-NMR peak intensities between the proton peaks of *N*-acetylated units of CS and imidazole group of histidine. It was found that the degree of replacement of H6R6 peptide on the CS molecule was approximately 1.2%.

Preparation and characterization of H6R6-NP

H6R6-NP was constructed by complex coacervation method. First, H6R6-CS copolymer was dissolved in 1 mg/mL of acetate solution. In this slightly acidic environment, H6R6-CS copolymer had a positive charge and reacted with negatively charged siRNA by electrostatic interaction, and as a result
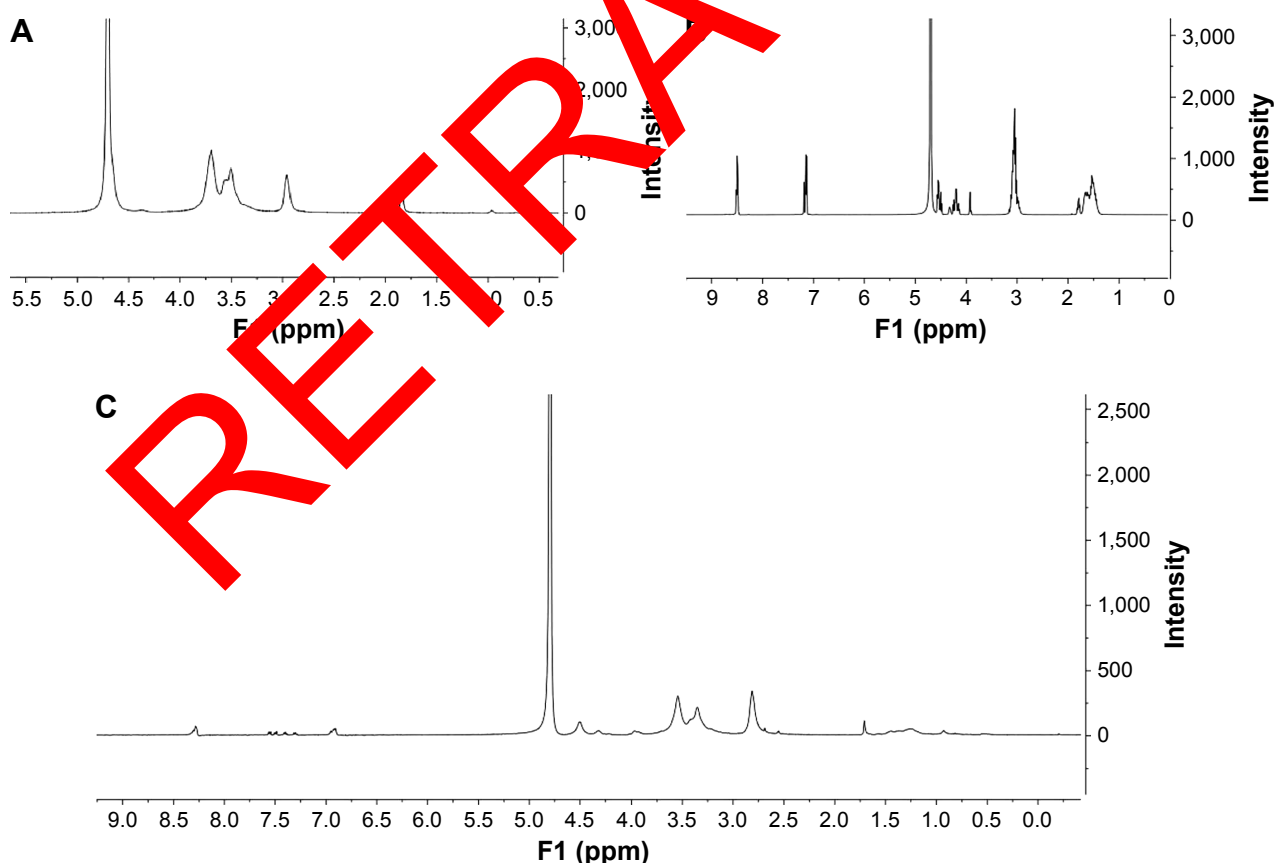

Figure 2 The ¹H-NMR spectra of CS (**A**), H6R6 peptide (**B**), and H6R6-CS copolymer (**C**).
Abbreviations: CS, chitosan; H6R6, poly(histidine-arginine)₆; H6R6-CS, poly(histidine-arginine)₆-modified chitosan.

NPs with high encapsulating efficiency were formed. The average particle size of H6R6-NP was 175 nm (PDI =0.25) (Figure 3A) and the ζ potential was +14.8 (Figure 3B). These indicate that the NP surfaces are surrounded by H6R6-CS polymers with positive charge, and H6R6-NP exhibited a spherical-shaped and smooth surface morphology with smaller particle size (Figure 3C). In addition, gel retardation was performed to assess the binding capacity of copolymers to the siRNAs (Figure 3D). The results showed that the H6R6-CS copolymer effectively condensed with siRNA at a weight ratio of 100:1, suggesting that H6R6-CS had preferable siRNA loading capacity.

Proliferation inhibition effect of H6R6-NP

The cytotoxic effect of H6R6-CS copolymer on tumor cells 4T1 and B16-F10 was assessed by MTT method. The cell viability ratio in various groups was observed to be more than 90% at concentrations ranging from 5 μg/mL to 80 μg/mL, which indicates that H6R6-CS copolymer had no distinct cytotoxic effect on these two tumor cells after 48 h of incubation (Figure 4A and B). This result emphasizes that H6R6-CS copolymer can be used as a safe carrier for delivering siRNA.

The H6R6-NP for delivering the targeting survivin siRNA significantly inhibited the proliferation of 4T1 cells. The cell viability ratio of 4T1 cells treated with H6R6-NP at a concentration of 5 pmol/well was remarkably lower than that of other groups. Furthermore, H6R6-NP exhibited time-dependent cytotoxic effects. The cell viability ratio of H6R6-NP group after 48 h of incubation was significantly lower than that after 24 h of incubation (Figure 4C). In addition, 4T1 cells were treated with free siRNA, CS-NP, H6R6-NP, and Liposome 2000, respectively. The cell viability ratio in each group differed. Free siRNA and CS-NP groups exhibited a low inhibitory effect and the cell viability ratio was 83% and 72%, respectively. Whereas the cell viability ratio was 54% in H6R6-NP groups and showed an obvious inhibitory effect in vitro compared to other groups (Figure 4D), for example, the positive group Liposome 2000. This result suggests that siRNA encapsulated with H6R6-CS polymer has as an excellent therapeutic effect on 4T1 cells.

Effect of H6R6-NP in inducing apoptosis

The ability of H6R6-NP to induce apoptosis and to cause necrosis in 4T1 cells was analyzed by Annexin-V-FITC/PI test. Annexin-V-FITC, a binding protein, can bind with
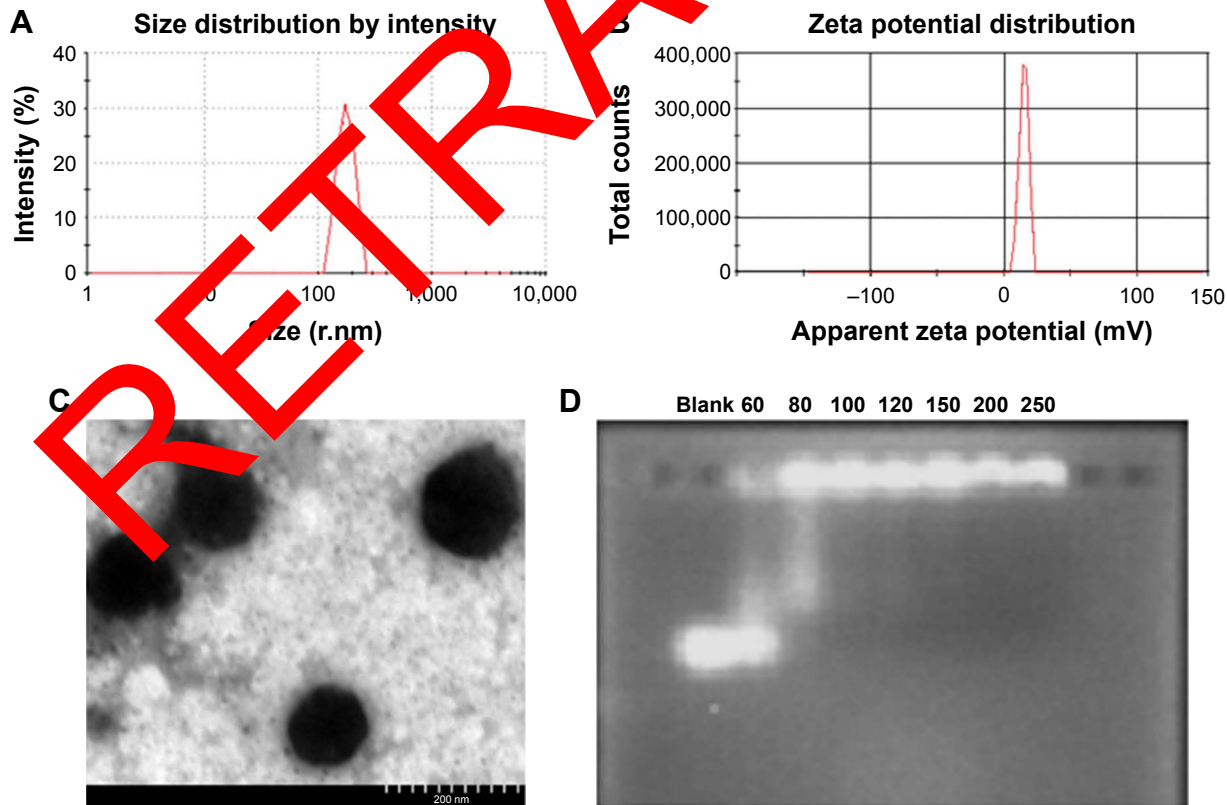

Figure 3 The characterization of H6R6-NP. (**A**) Size distribution; (**B**) zeta potential distribution; (**C**) TEM images of H6R6-NP (scale bar was 200 nm); and (**D**) agarose gel electrophoresis of H6R6-NP prepared at weight ratios ranging from 60:1 to 250:1.
Abbreviations: H6R6-NP, poly(histidine-arginine)$_6$-modified chitosan/siRNA nanoparticles; TEM, transmission electron microscopy.
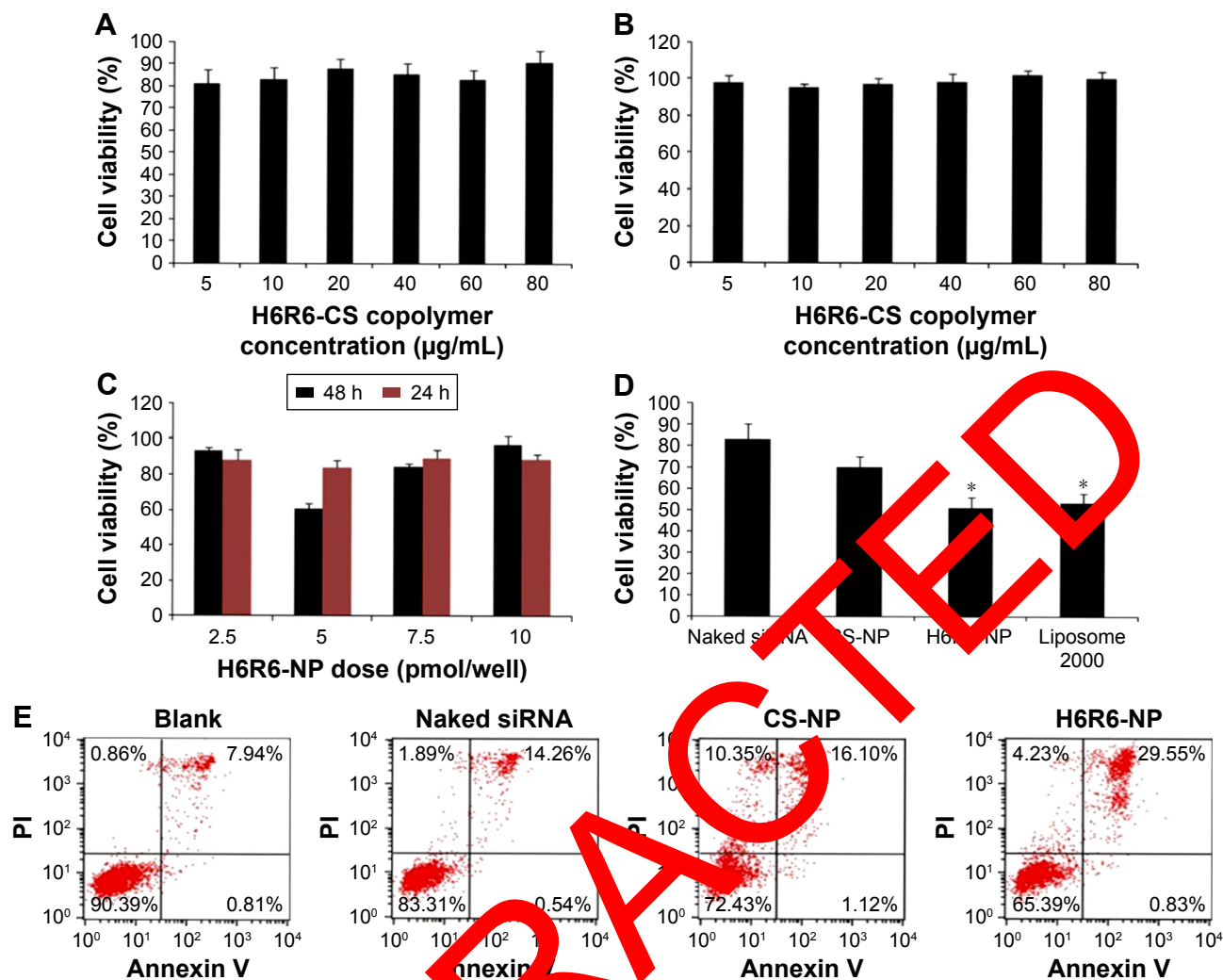
Figure 4 MTT assay and apoptosis analysis by flow cytometry. ~~toxic~~ effect of H6R6-CS copolymer on (**A**) 4T1 cells at a concentration of 5–80 μg/mL and on (**B**) B16–F10 at a concentration of 5–80 μg/mL. (**C**) The anti-proliferative effect of H6R6-NP on 4T1 cells at the siRNA dose 2.5–10 pmol/well for incubating 24 h and 48 h. (**D**) The anti-proliferation effect of H6R6-NP on 4T1 cells after 48 h of incubation at a dosage of 5 pmol/well; naked siRNA and CS-NP were taken as controls and Liposome 2000 was taken as positive control. Data are expressed as means ± SD, n>3. *$P<0.05$ vs Naked siRNA group and CS-NP group (calculated by Student's *t*-test). (**E**) Apoptosis ratio of 4T1 cells treated with naked siRNA, CS-NP, and H6R6-NP. Cells that did not undergo any treatment were used as blank.
Abbreviations: H6R6-NP, poly(histidine-arginine)$_6$-modified chitosan/siRNA nanoparticles; H6R6-CS, poly(histidine-arginine)$_6$-modified chitosan; siRNA, small interfering RNA; CS-NP, chitosan nanoparticles.

phosphatidyl serine and can translocate from inner to outer leaflet of cell membranes, whereas PI can enter necrosis cells easily. The combined application of Annexin-V-FITC and PI helps in distinguishing normal from necrosis cells. Annexin-V-FITC/PI was used to stain the 4T1 cells after treatment with various formulations containing the dose of 200 pmol therapeutic siRNA for transfection 48 h, and then were analyzed by flow cytometer. The apoptotic rate of 4T1 cells treated with PBS (blank group) and free siRNA was lower, about 8% and 14%, respectively, whereas those of the cells treated with CS-NP was higher (about 17%). This emphasizes that CS-NP has a slight apoptosis-inducing effect as CS protects siRNA from degradation. While in the H6R6-NP group, the apoptotic rate was 30%, which is significantly higher than

that of the other groups (Figure 4E). This result demonstrates that H6R6-NP induced apoptosis remarkably due to its high transfection efficiency.

Antimigration effect of H6R6-NP

The antimigration effect of H6R6-NP on 4T1 tumor cells was evaluated by wound-healing assay. The results are shown in Figure 5. At 24 h of incubation, scratch wound was clearly visible in every group, while at 48 h of incubation, the wound in blank and naked siRNA groups was almost closed and overlapped completely. This result implies that 4T1 cells proliferated rapidly in these two groups; however, in CS-NP and H6R6-NP groups, obvious wound was observed due to the antimigration function of the NPs. Moreover,
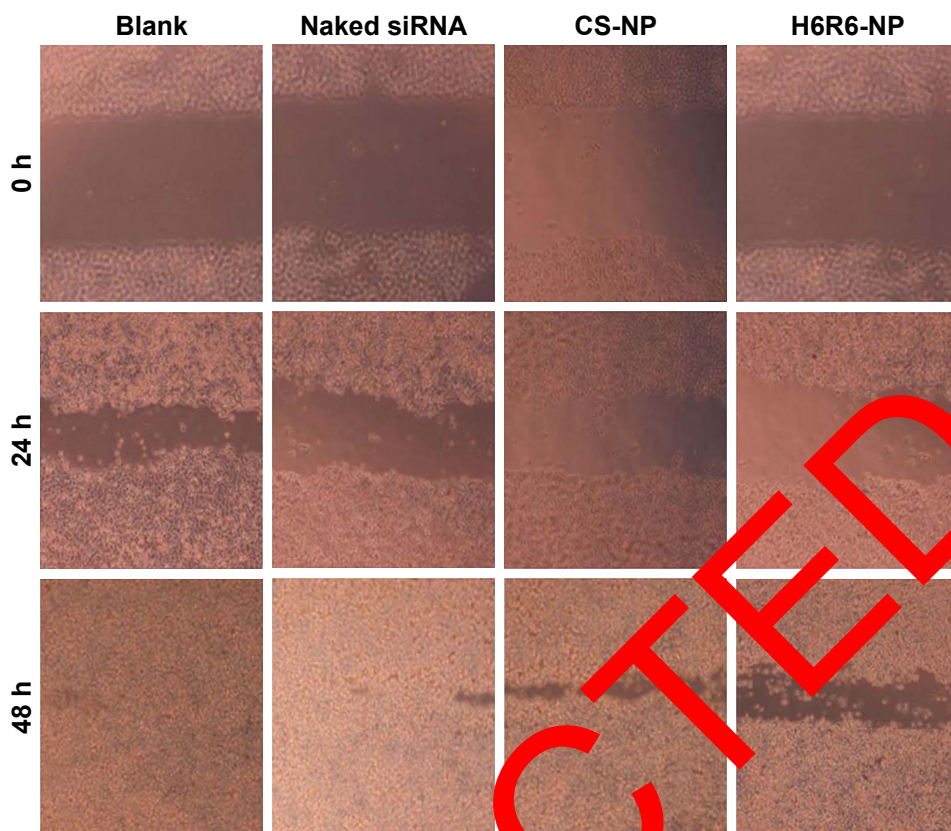
Figure 5 Wound-healing assay of H6R6-NP on 4T1 cells. 4T1 cells were treated with naked siRNA, CS-NP, and H6R6-NP and incubated for 48 h. Cells that did not undergo any treatment were used as blank. Wound healing was observed at 0 h, 24 h, and 48 h using an inverted microscope.
Abbreviations: H6R6-NP, poly(histidine-arginine)₆-modified chitosan/siRNA nanoparticle; siRNA, small interfering RNA; CS-NP, chitosan nanoparticle.

the scratch-wound area was wider in H6R6-NP group compared to CS-NP. This result suggests that H6R6-NP could inhibit 4T1 cell migration effectively compared to CS-NP.

Uptake study and endosomal esacpe effect

The uptake ability of H6R6-NP in vitro was evaluated by flow cytometry and CLSM (Figure 6). We prepared NPs encapsulated with siRNA-FAM before the start of the experiment, which can be quantified approximately. According to our theory, the cellular uptake of H6R6-NP is expected to increase due to the cell penetrating effect of R6. Once the NPs enter into the cells, they get trapped and escape from endosome/lysosome because of the protonation of imidazole ring present in histidine. As a result the release of siRNA into cytoplasm gets increased and the treatment effect gets enhanced further.

As shown in Figure 6A, the uptake efficiency of cells treated with naked siRNA and CS-NP was low, and uptake curve showed a slight shift in these two groups. In contrast, the uptake curve of the H6R6-NP group shifted to the right compared to that of the naked siRNA and CS-NP groups. Two peaks appeared in different position, and this

phenomenon ascribed that the substitute degree of H6R6 on the CS was uneven. These results indicate that H6R6-NP could be internalized easily and thus enhance fluorescence intensity. These results also reveal that H6R6-CS copolymer can deliver siRNA into the tumor cells effectively compared to CS-NP. This conclusion was further verified by CLSM test. To further investigate the intracellular distribution of H6R6-NP in 4T1 tumor cells, the siRNA (FAM labelled) was selected to prepare the drug-loading nanoparticle, the FAM labeled siRNA merged a green fluorescence at 488 nm. After 4 h of transfection, the green fluorescence was almost invisible naked siRNA-FAM group, and the fluorescence was quite weak in CS-NP group. This indicates that naked siRNA-FAM and CS-NP could not enter the tumor cells. In contrast, when siRNA-FAM was delivered via H6R6-CS copolymer, H6R6-NPs were found inside the cytoplasm of the 4T1 cells and showed a higher internalization compared to free siRNA and CS-NP. Taken together, the results of this study reveal that H6R6-NP is internalized by tumor cells easily (Figure 6B).

The endosome/lysosome escape capacity of H6R6-NP was estimated by treating 4T1 cells with CS-NP and H6R6-NP,
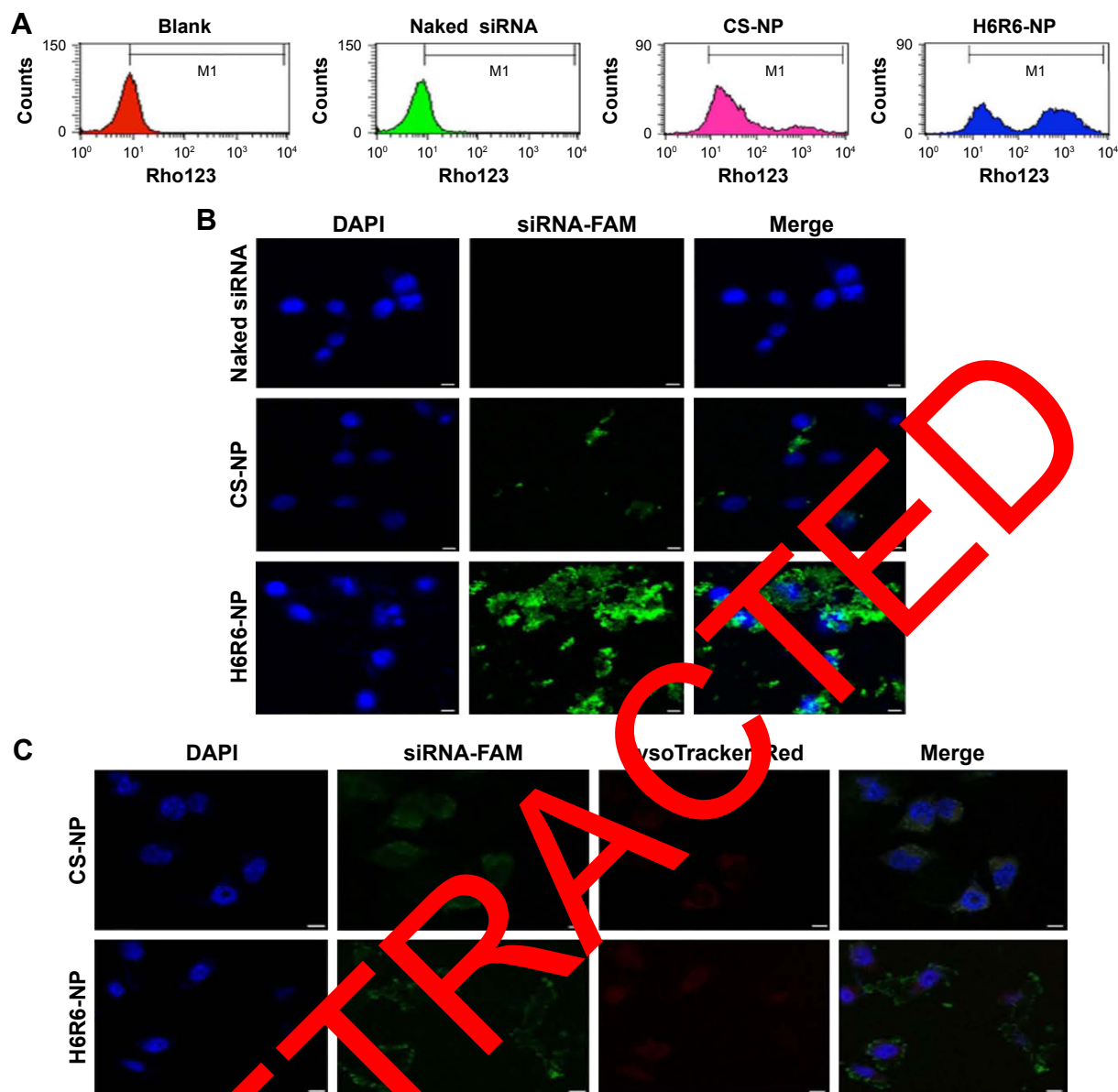
Figure 6 Uptake effect and endosomal escape effect in 4T1 cells were determined by flow cytometry and CLSM. (**A**) Cellular uptake behavior was studied by flow cytometer; cells that did not undergo any treatment were used as blank; (**B**) CLSM images of 4T1 cells incubated with naked siRNA, CS-NP, and H6R6-NP. Cell nuclei were stained with DAPI (blue), and siRNA was labeled by FAM (green fluorescence), the scale bar was 8 µm; (**C**) The study of the endosomal escape effect of the H6R6-NP, and the CS-NP was control group; cytoplasmes and cell nuclei were stained with cell Navigator™ Lysosome Staining Kit (red) and DAPI (blue), respectively; siRNA-FAM formed green fluorescence. Scale bar was 8 µm.
Abbreviations: H6R6-NP, poly (histidine-arginine)$_6$-modified chitosan/siRNA nanoparticles; siRNA, small interfering RNA; CS-NP, chitosan nanoparticle; CLSM, confocal laser scanning microscopy.

respectively. The cells were then observed using confocal microscope. The endosomes/lysosomes stained with cell Navigator Lysosome Staining Kit formed a deep red fluorescence, and siRNAs stained with FAM formed a green fluorescence. The cell nucleus appeared blue fluorescent on staining with DAPI. When the NPs were trapped in the endosomes/lysosomes, the green fluorescence and red fluorescence overlapped to show a yellow fluorescence around the cell nucleus. After 6 h of incubation, in CS-NP group, siRNA-FAMs (green) were

homogeneously surrounded by lysosomes/endosomes (red). The green siRNA-FAM and red lysosomes/endosomes merged to form a yellow fluorescence, which suggested that CS-NP accumulated within lysosomes/endosomes after 6 h of transfection. The H6R6-CS/siRNA nanoparticle (green fluorescence labeled) appeared around the cell nucleus and was clearly separated with the red fluorescence from lysosomes/endosomes, which indicated that the nanoparticle was distinctly got away from lysosomes/endosomes (red fluorescence labelled) (Figure 6C).

Thus we concluded that H6R6-CS had significant buffering capacity and could assist siRNA to escape from lysosomes/endosomes. This phenomenon attributed to the protonation of imidazole resulting in "proton sponge effect", which in turn could rupture the lysosomes/endosomes membrane to release siRNA into cytoplasm.

Results of animal experiments

For investigating the therapeutic effect of H6R6-NP on breast cancer, tumor-bearing mouse model was established to inject 4T1[luc] into the orthotopic mammary site of female BALB/c mice. In blank group an increased tumor growth was observed, which emphasizes that H6R6-NP had no inhibitory effect on breast tumor cells. Whereas in free siRNA group, the tumor growth was relatively low, which suggests that free siRNA had a slight inhibitory effect on tumor cells. In the test groups, a sharp decrease in tumor growth was observed, which shows that H6R6-NP had a remarkable inhibitory effect on tumor cells (Figure 7A).

At the end of the experiment, the solid tumors were excised from the tumor-bearing mice and weighed to investigate the antitumor effect. A significant decrease in the tumor weight was observed in the test group compared to the blank and free siRNA groups (Figure 7B and C). This result suggests that H6R6-NP had a significant inhibitory effect on the tumor growth of 4T1 cells, and this finding was consistent with that found in previous literature.[41,42] This phenomenon ascribes that H6R6-CS copolymer as a non-viral vector can be used to encapsulate siRNA effectively to form a stable NP, which protects siRNA from being degraded by nuclease in tumor tissues. Moreover, H6R6-NP possessed higher membrane-penetrating capacity and better endosomal escape effect. As a result, a large amount of therapeutic siRNA could be released into the cytoplasm, thereby increasing the treatment efficacy. The survival curves of mice in various group are shown in Figure 7D. The mice in blank group were dead on the 38th day after inoculating tumor cells and those treated with naked siRNA had a slight prolonged survival time, but
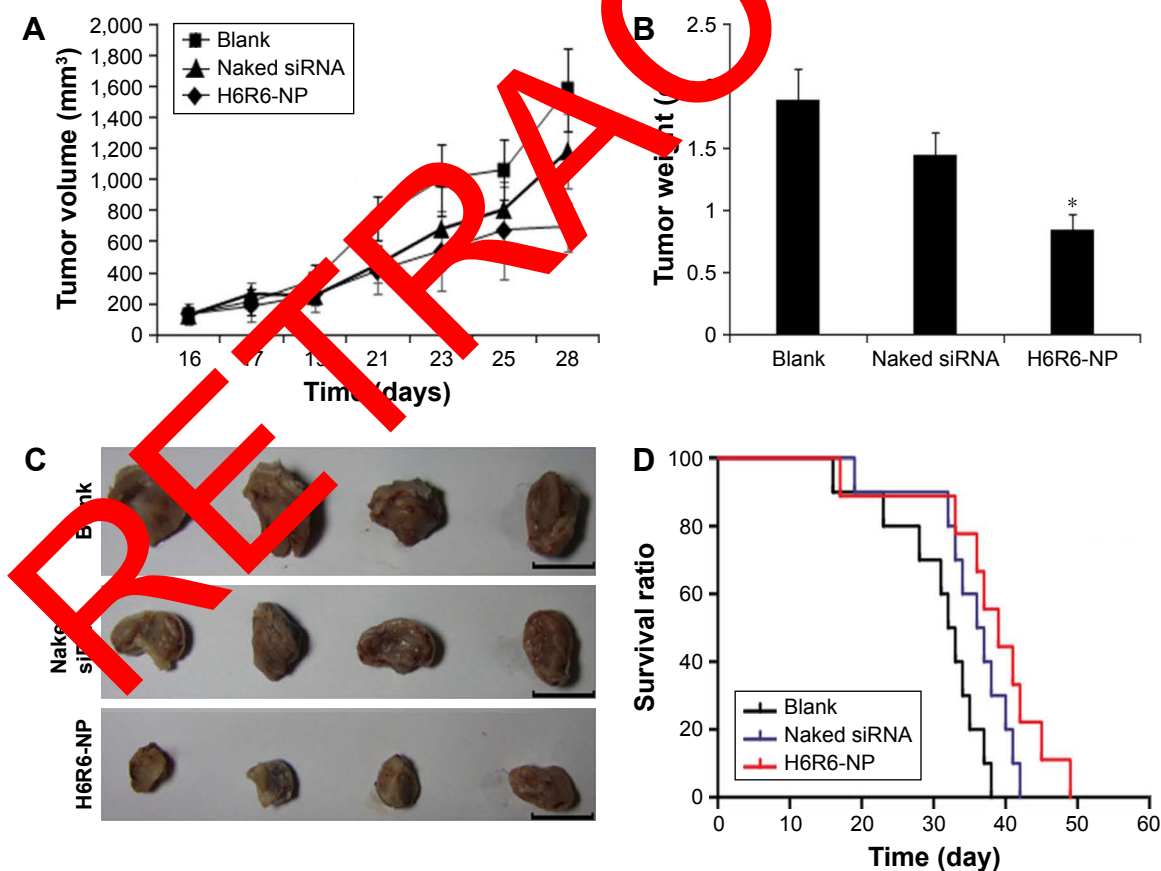

Figure 7 The inhibitory effect of H6R6-NP on 4T1 tumor cells. (**A**) Tumor volume was measured every other day in tumor-bearing mice. (**B**) Tumor was exfoliated and weighed. The data was mean ± SD, n=5. (**C**) Photographs of tumor in blank group, naked siRNA group, and H6R6-NP group. Scale bar =20 mm. (**D**) The survival curve of tumor-bearing mice injected with naked siRNA and H6R6-NP, respectively; n=10; the blank group was treated with saline. *$P < 0.05$ vs blank group and naked siRNA group.
Abbreviations: H6R6-NP, poly(histidine-arginine)$_6$-modified chitosan/siRNA nanoparticles; siRNA, small interfering RNA; SD, standard deviation.

they died 42 days after administration. These results indicate that free siRNA had a low therapeutic effect on tumor-bearing mice, and all mice in test group treated with H6R6-NP survived for 49 days. Based on these results, we concluded that H6R6-NP can significantly prolong the survival time of tumor-bearing mouse.

As we all know, 4T1 breast cancer was highly invasive, and typically shift to the lung and liver in tumor-bearing mice. At the end of the experiment, tumor tissues were isolated from the lungs of tumor-bearing mice and photographed by a digital camera. The photograph (Figure 8A) shows that a plenty of white nodules were observed on the surface of lung lobe in blank and free siRNA groups, and no white nodules were observed in the test group. Presence of white nodules on the surface of lung lobe is an important symbol of 4T1

cell metastasis. In both blank and free siRNA groups, 4T1 cell metastasis was observed compared to test group, and a smaller metastasis scope in test group imply that H6R6-NP can hamper 4T1 tumor cells metastasis.

In addition, lung and liver tissues were stained with H&E for histopathological analysis. A large area of metastatic focus was found in the pathological lung tissues in blank group and naked siRNA groups. The morphology of the pathological slices of the test group was similar to that of healthy mice (Figure 8B), which showed a distinct difference in lung structure and alveolar septum. Results of liver histopathological analysis show that a large number of metastatic sites were found in the liver pathological slices in the blank and naked siRNA groups; however, in the test group, only few metastatic spots were found, and the hepatic tissues
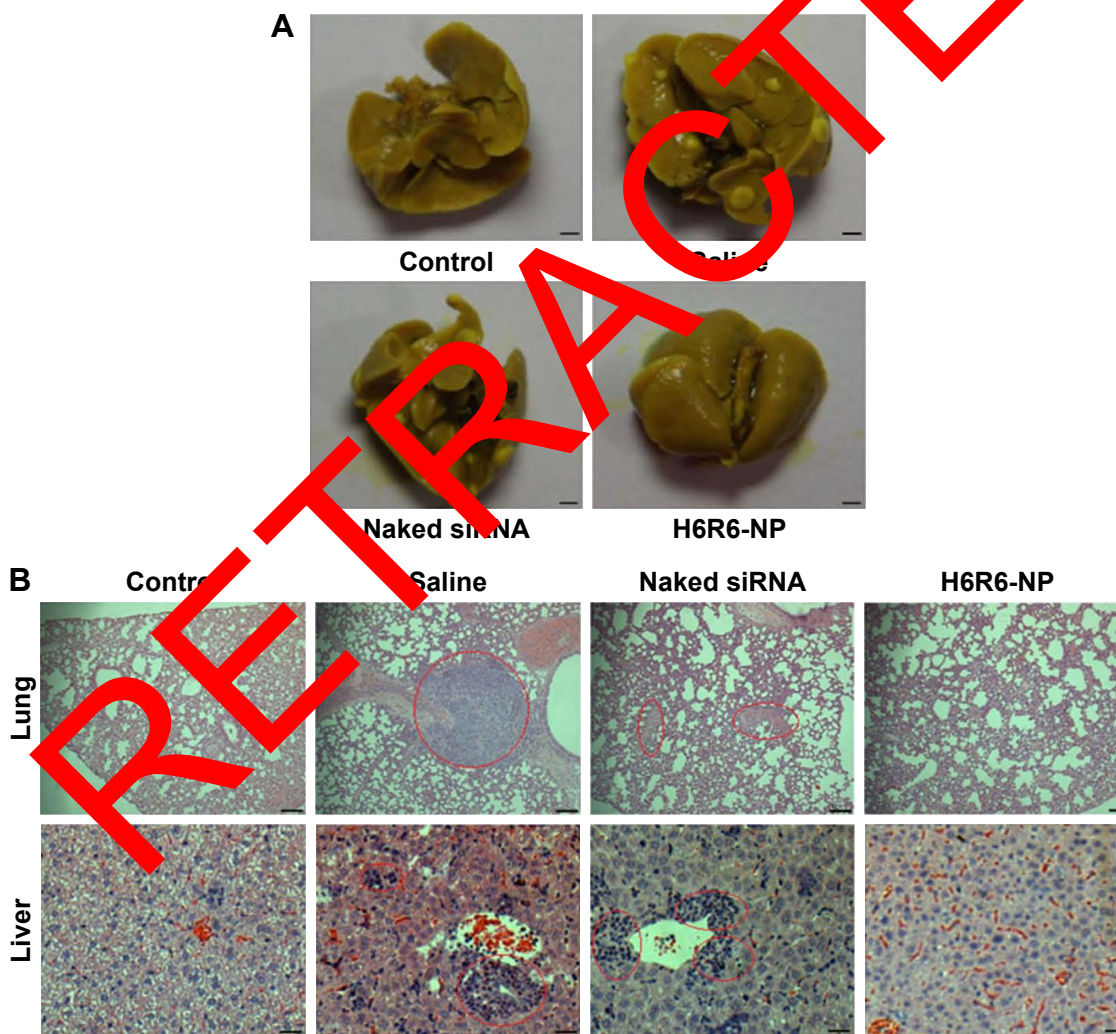

Figure 8 The suppression effect of H6R6-NP on cancer metastasis. (**A**) Images of lungs of tumor-bearing mice respectively treated with normal saline, naked siRNA, and H6R6-NP. Healthy mice were used as blank. Mice treated with saline and naked siRNA were used as negative control; scale bar =5 mm. (**B**) H&E-stained lung and liver sections of 4T1-bearing mice treated with saline, naked siRNA, and H6R6-NP. Lung and liver tissues from normal mice were taken as control; scale bar =12 μm.
Abbreviations: H6R6-NP, poly(histidine-arginine)₆-modified chitosan/siRNA nanoparticles; siRNA, small interfering RNA; H&E, hematoxylin and eosin.

appeared similar to that of the normal mice (Figure 8B). Therefore, we concluded that tumor-bearing mice in blank and naked siRNA groups could not resist metastasis easily and the mice in test group could resist tumor metastasis effectively. These results demonstrate that H6R6-NP could inhibit 4T1 cell metastasis significantly; this conclusion is in accordance with previous reports.[43–45]

Conclusion

Multifunctional H6R6-CS copolymers were prepared by linking H6R6 peptide and CS to overcome its low cellular uptake efficiency and poor endosomal escape ability for siRNA delivery. The results showed that introduction of H6R6 peptide into CS molecule increased its internalization efficiency and buffering capacity significantly. H6R6-NP possessed endosomal escape effect in vitro cell experiment, led to H6R6-NP escape from the endosomes rapidly and release siRNA into the cytoplasm effectively. Moreover, H6R6-NP can markedly inhibit the growth and metastasis of the tumor cells in vitro and in vivo. Thus, H6R6-CS copolymer is an outstanding vector for siRNA delivery and has tremendous potential to application in breast tumor therapy. We hope that future research will focus on H6R6-CS copolymer in developing it as a perfect carrier for intravenous siRNA delivery and in emphasizing H6R6-NP as a promising candidate to be applied in clinical settings for breast cancer therapy.

Acknowledgments

Disclosure

The authors declare no conflicts of interest in this work.

Reference

1. Jafarian N, Kuppler K, Rosa M, Hoover S, Patel B. Chronic lymphocytic leukemia and invasive ductal carcinoma presenting as a collision breast tumor. *Clin Breast Cancer*. 2015;15(4):e209–e212.
2. Li M, Zhang J, Ouyang T, et al. Incidence of BRCA1 somatic mutations and response to neoadjuvant chemotherapy in Chinese women with triple-negative breast cancer. *Gene*. 2016;584(1):26–30.
3. Nastiuk KL, Krolewski JJ. Opportunities and challenges in combination gene cancer therapy. *Adv Drug Deliver Rev*. 2016;98:35–40.
4. Karjoo Z, Chen XG, Hatefi A. Progress and problems with the use of suicide genes for targeted cancer therapy. *Adv Drug Deliv Rev*. 2016; 99(Pt A):113–128.
5. Salzano G, Riehle R, Navarro G, Perche F, De Rosa G, Torchilin VP. Polymeric micelles containing reversibly phospholipid-modified anti-survivin siRNA: a promising strategy to overcome drug resistance in cancer. *Cancer Lett*. 2014;343(2):224–231.
6. Nestal de Moraes G, Delbue D, Silva KL, et al. FOXM1 targets XIAP and survivin to modulate breast cancer survival and chemoresistance. *Cell Signal*. 2015;27(12):2496–2505.
7. Dai G, Zheng W, Ma X, Wang P. Multisite mutation of monomer survivin with enhanced effect on apoptosis regulation of breast cancer cells. *Biomed Pharmacother*. 2015;69:111–118.
8. Conde J, Ambrosone A, Hernandez Y, et al. 15 years on siRNA delivery: beyond the state-of-the-art on inorganic nanoparticles for RNAi therapeutics. *Nano Today*. 2015;10(4):421–450.
9. Gao J, Liu W, Xia Y, et al. The promotion of siRNA delivery to breast cancer overexpressing epidermal growth factor receptor through anti-EGFR antibody conjugation by immunoliposomes. *Biomaterials*. 2011; 32(13):3459–3470.
10. Lee SJ, Kim MJ, Kwon IC, Roberts TM. Delivery strategies and potential targets for siRNA in major cancer types. *Adv Drug Deliver Rev*. 2016; 104:2–15.
11. Zhi D, Zhao Y, Cui S, Chen H, Zhang S. Conjugates of small targeting molecules to non-viral vectors for the mediation of siRNA. *Acta Biomater*. 2016;36:21–41.
12. Han L, Tang C, Yin C. Enhanced antitumor efficacies of multifunctional nanocomplexes through knocking down the barriers for siRNA delivery. *Biomaterials*. 2015;44:111–121.
13. Park EY, Jang M, Kim JH, Ahn HJ. Genetically modified *Tomato aspermy virus* 2b protein as a tumor-targeting siRNA delivery carrier. *Acta Biomater*. 2014;10(11):4778–4786.
14. Guo J, Cahill MR, McKenna SL, O'Driscoll CM. Biomimetic nanoparticles for siRNA delivery in the treatment of leukaemia. *Biotechnol Adv*. 2014;32(8):1396–1409.
15. Bus T, Cheng Q, Jiang Q, et al. Enhanced endosomal/lysosomal escape by distearoyl phosphoethanolamine-polycarboxybetaine lipid for systemic delivery of siRNA. *J Control Release*. 2014;176:104–114.
16. Ragelle H, Vandermeulen G, Préat V. Chitosan-based siRNA delivery systems. *J Control Release*. 2013;172(1):207–218.
17. Corbet C, Ragelle H, Pourcelle V, et al. Delivery of siRNA targeting tumor metabolism using non-covalent PEGylated chitosan nanoparticles: identification of an optimal combination of ligand structure, linker and grafting method. *J Control Release*. 2016;223:53–63.
18. Vauthier C, Zandanel C, Ramon AL, et al. Chitosan-based nanoparticles for in vivo delivery of interfering agents including siRNA. *Curr Opin Colloid Interface Sci*. 2013;18(5):406–418.
19. Deng ZJ, Morton SW, Bonner DK, Gu L, Ow H, Hammond PT. A plug-and-play ratiometric pH-sensing nanoprobe for high-throughput investigation of endosomal escape. *Biomaterials*. 2015;51:250–256.
20. Martens TF, Remaut K, Demeester J, De Smedt SC, Braeckmans K. Intracellular delivery of nanomaterials: how to catch endosomal escape in the act. *Nano Today*. 2014;9(3):344–364.
21. Xiao B, Ma P, Viennois E, Merlin D. Urocanic acid-modified chitosan nanoparticles can confer anti-inflammatory effect by delivering CD98 siRNA to macrophages. *Colloid Surf B Biointerfaces*. 2016;143: 186–193.
22. Shi B, Zhang H, Bi J, Dai S. Endosomal pH responsive polymers for efficient cancer targeted gene therapy. *Colloid Surf B Biointerfaces*. 2014;119:55–65.
23. Liu X, Mo Y, Liu X, et al. Synthesis, characterisation and preliminary investigation of the haemocompatibility of polyethyleneimine-grafted carboxymethyl chitosan for gene delivery. *Mater Sci Eng C Mater Biol Appl*. 2016;62:173–182.
24. Thomas A, Lins L, Divita G, Brasseur R. Realistic modeling approaches of structure-function properties of CPPs in non-covalent complexes. *Biochim Biophys Acta*. 2010;1798(12):2217–2222.
25. Veiman KL, Künnapuu K, Lehto T, et al. PEG shielded MMP sensitive CPPs for efficient and tumor specific gene delivery in vivo. *J Control Release*. 2015;209:238–247.

26. Bass J. CPP magnetoresistance of magnetic multilayers: a critical review. *J Magn Magn Mater*. 2016;408:244–320.

27. Park K. Arginine-rich CPPs for improved drug delivery to tumors. *J Control Release*. 2012;159(2):153.

28. Kato T, Yamashita H, Misawa T, et al. Plasmid DNA delivery by arginine-rich cell-penetrating peptides containing unnatural amino acids. *Bioorg Med Chem*. 2016;24(12):2681–2687.

29. Shirazi AN, El-Sayed NS, Mandal D, et al. Cysteine and arginine-rich peptides as molecular carriers. *Bioorg Med Chem Lett*. 2016;26(2): 656–661.

30. Ronca F, Raggi A. Structure-function relationships in mammalian histidine-proline-rich glycoprotein. *Biochimie*. 2015;118:207–220.

31. Chou ST, Hom K, Zhang D, et al. Enhanced silencing and stabilization of siRNA polyplexes by histidine-mediated hydrogen bonds. *Biomaterials*. 2014;35(2):846–855.

32. Wen Y, Guo Z, Du Z, et al. Serum tolerance and endosomal escape capacity of histidine-modified pDNA-loaded complexes based on polyamidoamine dendrimer derivatives. *Biomaterials*. 2012;33(32):8111–8121.

33. Liu BR, Huang YW, Winiarz JG, Chiang HJ, Lee HJ. Intracellular delivery of quantum dots mediated by a histidine- and arginine-rich HR9 cell-penetrating peptide through the direct membrane translocation mechanism. *Biomaterials*. 2011;32(13):3520–3537.

34. Moreira C, Oliveira H, Pires LR, Simões S, Barbosa MA, Pêgo AP. Improving chitosan-mediated gene transfer by the introduction of intracellular buffering moieties into the chitosan backbone. *Acta Biomater*. 2009; 5(8):2995–3006.

35. Corbet C, Ragelle H, Pourcelle V, et al. Delivery of siRNA targeting tumor metabolism using non-covalent PEGylated chitosan nanoparticles: identification of an optimal combination of ligand structure, linker and grafting method. *J Control Release*. 2016;223:53–63.

36. Yang F, Huang W, Li Y, et al. Anti-tumor effects in mice induced by survivin-targeted siRNA delivered through polysaccharide nanoparticles. *Biomaterials*. 2013;34(22):5689–5699.

37. Cui M, Au JL, Wientjes MG, O'Donnell MA, Loughlin KR, Lu Z. Intravenous siRNA silencing of survivin enhances activity of mitomycin C in human bladder RT4 xenografts. *J Urol*. 2015;194(1):230–237.

38. Rahmani S, Mohammadi Z, Amini M, et al. Methylated 4-N,N dimethyl aminobenzyl N,O carboxymethyl chitosan as a new chitosan derivative: synthesis, characterization, cytotoxicity and antibacterial activity. *Carbohyd Polym*. 2016;149:131–139.

39. Bygd HC, Akilbekova D, Muñoz A, Forsmark KD, Bratlie KM. Poly-L-arginine based materials as instructive substrates for fibroblast synthesis of collagen. *Biomaterials*. 2015;63:47–57.

40. Al-Maythalony BA, Isab AA, Wazeer MI, Ibdah A. Investigation of the interaction of gold(III)–alkyldiamine complexes with L-histidine and imidazole ligands by ^{1}H and ^{13}C NMR, and UV spectrophotometry. *Inorg Chim Acta*. 2010;363(13):3200–3207.

41. Liu S, Huang W, Jin MJ, Fan B, Xia GM, Gao ZG. Inhibition of murine breast cancer growth and metastasis by survivin-targeted siRNA using disulfide cross-linked linear PEI. *Eur J Pharm Sci*. 2015;82:171–182.

42. Tang S, Yin Q, Su J, et al. Inhibition of metastasis and growth of breast cancer by pH-sensitive poly (β-amino ester) nanoparticles co-delivering two siRNA and paclitaxel. *Biomaterials*. 2015;48:1–15.

43. Zhao P, Xia G, Dong S, Jiang ZX, Chen M. An iNGR-derived and PEP-salinomycin nanoparticle that specifically and effectively inhibits metastases of 4T1 orthotopic breast tumors. *Biomaterials*. 2016;93:1–9.

44. Luo KW, Yue GG, Ko CH, et al. In vivo and in vitro anti-tumor and anti-metastatic effects of Coriolus versicolor aqueous extract on mouse mammary 4T1 carcinoma. *Phytomedicine*. 2014;21(8–9):1078–1087.

45. Kim YJ, Bae J, Shin TH, et al. Immunoglobulin Fc-fused, neuropilin-1-specific peptide shows efficient tumor tissue penetration and inhibits tumor growth via anti-angiogenesis. *J Control Release*. 2015; 216:56–68.